NONLINEAR THERMOMECHANICAL MODELING OF REFRACTORY MASONRY LININGS WITH DRY JOINTS

Mahmoud Mahmoud Alaa Ali, Thomas Sayet, Alain Gasser, Eric Blond

▶ **To cite this version:**

Mahmoud Mahmoud Alaa Ali, Thomas Sayet, Alain Gasser, Eric Blond. NONLINEAR THERMOMECHANICAL MODELING OF REFRACTORY MASONRY LININGS WITH DRY JOINTS. Unified International Technical Conference on Refractories (UNITECR 2022), Mar 2022, Chicago, United States. hal-03633355

HAL Id: hal-03633355
https://hal.science/hal-03633355v1

Submitted on 7 Apr 2022

HAL is a multi-disciplinary open access archive for the deposit and dissemination of scientific research documents, whether they are published or not. The documents may come from teaching and research institutions in France or abroad, or from public or private research centers.

L'archive ouverte pluridisciplinaire **HAL**, est destinée au dépôt et à la diffusion de documents scientifiques de niveau recherche, publiés ou non, émanant des établissements d'enseignement et de recherche français ou étrangers, des laboratoires publics ou privés.

NONLINEAR THERMOMECHANICAL MODELING OF REFRACTORY MASONRY LININGS WITH DRY JOINTS

Mahmoud Ali*, Thomas Sayet, Alain Gasser, and Eric Blond
LaMé laboratory (EA 7494), Université d'Orléans, Université de Tours, INSA Centre Val de Loire, 8 rue Léonard de Vinci, 45072 Orléans, France

ABSTRACT

In many high temperature industries, including iron and steel industry, refractory masonry with dry joints is extensively used for lining the internal surfaces of several large-scale components such as steel ladles, rotary kilns, and furnaces. The normal operating conditions of these linings are high thermal gradients, thermal shock, slag attack, and high thermomechanical stresses. The design and optimization of these linings is still an engineering challenge due to the coupled interactions between thermal, mechanical, and chemical fields. Thus, advanced simulation techniques are necessary especially when experimental work is still a challenging task do to the harsh working conditions. Conventional simple macro models of these linings are in many cases not sufficient to predict the appropriate mechanical response. Micro modeling techniques must be resorted to, but these are known to be very expensive from the computational point of view. In this contribution, we propose a more efficient multi scale approach for the design and optimization of these linings. Nonlinear effects caused by progressive closure of dry joints and viscoplastic behavior of refractories at high temperature are accurately captured. Comparisons between experimental and numerical results of refractory masonry walls subjected to different loading conditions at room and high temperature are presented. Good agreements between the experimental and numerical results are obtained.

INTRODUCTION

In the steel-making industry, steel ladles are used as refining units and transportation vessels of liquid steel. They are composed of different refractory layers and steel construction components. The different layers include a working lining (layer in contact with liquid steel), a safety lining (also called permanent lining), insulation layers, and a steel shell. The working lining is usually made of refractory masonry with dry joints (in some cases it could be castable). While, the safety lining could be built up with refractory masonry with mortar joints (in some cases it could be castable). The refractory linings and the insulation layers insulate the steel shell from the liquid steel, reduce heat losses from the steel shell and, therefore, maintain the liquid steel temperature within the required limit. Among the different layers in the steel ladle, the working lining is the most critical layer due to being in direct contact with liquid steel. A well-designed working lining offers longer ladle's life time, better steel quality and productivity.

Finite Element (FE) based numerical models represent an efficient way to study, design and optimize large scale masonry structures with dry joints. Existing FE models could be classified as detailed micro modeling and multi scale models. Micro modeling approach provides accurate results as the detailed geometry of the bricks and the joints are separately modeled and, almost, all the information about the masonry components are taken into account. Within the framework of micro modeling, different models were developed such as those reported in [1–3]. They differ by the constitutive laws used to describe the behavior of dry joints and the physical models of joints. The majority of these models assumed rigid or purely elastic bricks and all material non-linearity is concentrated in the joints. The main limitations

of the micro modeling approach are related to huge computational time and solution convergence problems.

Multi scale modeling approach has a fair compromise between accuracy and computational cost, because the structural problem is usually divided into two scales: a homogeneous equivalent medium studied at the macroscopic scale with homogeneous properties determined by homogenizing the microscopic stress and strain fields in a carefully selected Representative Volume Element (RVE, microscopic scale). The homogenized properties are usually obtained using mechanical homogenization technique. Some examples of previous multi scale models of refractory masonry linings are reported in [3–5].

The present paper reports on large scale experimental characterization of refractory masonry with dry joints and computationally efficient multi scale models developed at University of Orleans - France. These validated models could help in predicting and understanding the complex thermomechanical behavior of refractory masonry and assist in their design and optimization.

EXPERIMENTAL CHARACTERIZATION

Several large-scale uniaxial and biaxial compression creep tests as well as biaxial relaxation tests of alumina spinel refractory masonry walls were performed. For all tests, the dimensions of the walls were 1125 x 1100 x 140 mm^3 and were built up with half and full cuboid bricks. The dimensions of the full bricks were 150$\times$ 100$\times$ 140 mm^3 (length, height, and depth) and the dimensions of the half bricks were 75$\times$ 100$\times$140 mm^3. The dimensional tolerances of the bricks were $\pm$ 2 mm in the pressing direction (150$\pm$2 mm) and $\pm$ 1 mm in the directions perpendicular to the pressing direction (100$\pm$1 mm and 140$\pm$1 mm). These tolerances lead to non-uniform joint thickness in the wall and limited initial contact.

A schematic of the experimental setup used to perform the biaxial compression tests of alumina spinel refractory masonry walls at room and high temperatures is shown in Figure 5. It is composed of a) a steel reaction frame with 3$\times$ 3$\times$1.6 m^3 size. b) Two hydraulic jacks with maximum stroke of 90 mm. c) Four steel plungers, two of them are fixed and the other two are moving. The two moving plungers are connected to the two hydraulic cylinders and equipped with lateral steel guides to ensure their alignment during load application. d) Plunger linings, built up with magnesia chromite bricks, installed inside the steel plungers. The alumina spinel walls were built in the test field and were surrounded by the moving and fixed plungers.

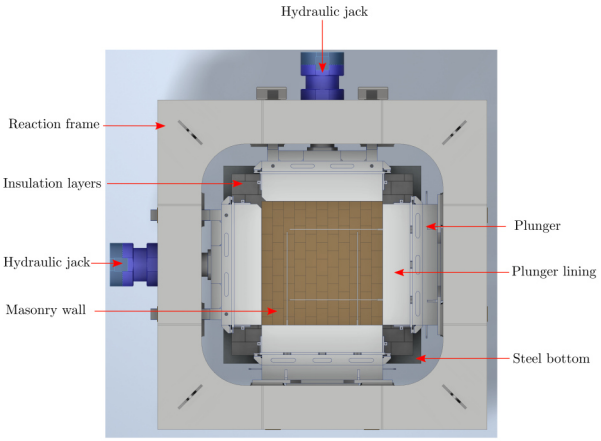

Figure 1: Top view of the biaxial compression test field.

For measuring the displacement, four alumina tubes and Linear Variable Differential Transformers (LVDTs) were used. In addition, Digital Image Correlation (DIC) was used to obtain the full displacement fields (at room temperature). In the high temperature tests, the temperatures of the cold and hot faces of the wall were measured thanks to several thermocouples. An example of refractory masonry specimen (before heating and testing) subjected to biaxial compression load at high temperature is given in Fig. 2.

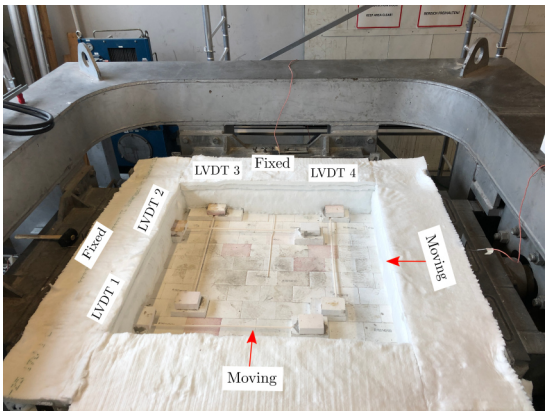

Figure 2: An example of refractory masonry wall subjected to biaxial compression at high temperature showing the arrangements of the LVDTs, moving and fixed plungers.

NUMERICAL MODELING

Refractory masonry with dry joints has strongly nonlinear stress-strain relationships due to gradual closure of joints and markedly orthotropic behavior (caused by the difference between the number of bed and head joints and the fact that they can be closed in one direction and open in the other direction). To numerically capture such nonlinear phenomena and consider the impacts of gradual joints closure/reopening on the homogenized mechanical response, four periodic joint patterns, as well as transition criteria between them, were defined as depicted in Fig. 3. Each pattern is associated with a specific state of bed and head joints (open or closed) and represents different periodic masonry structure with different equivalent elastic viscoplastic behavior. The predefined patterns are:

- Pattern C: head and bed joints are Closed (all joints are closed).
- Pattern B: Bed joints are closed, while head joints are open.
- Pattern H: Head joints are closed, while bed joints are open.
- Pattern O: head and bed joints are Open (all joints are open).

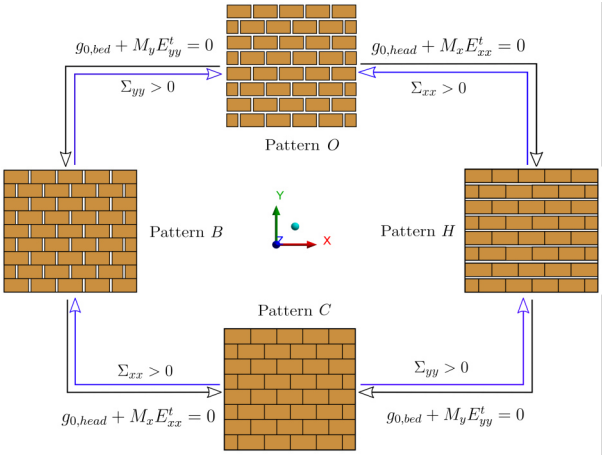

Figure 3: Schematics of all possible joint patterns of refractory masonry with dry joints and joints closure and reopening criteria.

The homogenized elastic viscoplastic behavior of each joint pattern is obtained using FE-base nonlinear homogenization technique. A Representative Volume Element (RVE) is selected from the periodic joint pattern. Next, combinations of uniaxial and simple shear loading simulations are performed on it. Then, the average stresses and strains are calculated by averaging the local stress and strain fields in the RVE. Finally, the homogenized elastic and viscoplastic tensors are obtained. Further details on the nonlinear homogenization analysis, identification of the homogenized elastic viscoplastic behavior of the four patterns and the transition criteria from one joint pattern to another are described in detail in references [4–8].

The homogenized elastic behavior of the four joint patterns can be described using the orthotropic forms of Hooke's law as [4, 7]:

$$\overline{\overline{\Sigma}} = \overline{\overline{\overline{\overline{C^e}}}} : \overline{\overline{E^e}} \tag{1}$$

Where $\overline{\overline{\Sigma}}$ and $\overline{\overline{E^e}}$ are the second order macroscopic stress and elastic strain tensors, while $\overline{\overline{\overline{\overline{C^e}}}}$ is the fourth order macroscopic elastic stiffness

tensor. $\overline{\overline{\overline{\overline{C^e}}}}$ of the four patterns is obtained using FE-based homogenization technique.

The orthotropic homogenized viscoplastic behavior of each pattern is obtained through averaging the local stress ($\overline{\overline{\sigma}}$), viscoplastic strain rate ($\overline{\overline{\dot{\varepsilon}^{\mathrm{vp}}}}$) and equivalent stress (σ_{eq}) fields over the volume of the RVE and using a localization tensor ($\overline{\overline{\overline{\overline{N}}}}$) according to:

$$\overline{\overline{\dot{E}^{vp}}} = \frac{1}{2} A \left(\Sigma_{eq}\right)^{n-1} \overline{\overline{\overline{\overline{N}}}} : \overline{\overline{\Sigma}} \tag{2}$$

Where A and n are creep parameters of the base material of the bricks, Σ_{eq} is the macroscopic equivalent stress. Tensor $\overline{\overline{\overline{\overline{N}}}}$ accounts for the orthotropy of the structure and enables using the creep parameters of the constitutive material (i.e. bridge between the micro and macro scales).

To consider the gradual increase in the effective stiffness with the gradual closure of joints and reproduce the strain stiffening behavior, the joints were reduced to an interface, at the RVE level - micro modeling (see Fig. 4), with small thickness (t_i) where the constitutive normal and shear behaviors of the joints have been implemented. The behavior law of the interface is expressed in an incremental form as:

$$\Delta\sigma = k(u)\,\Delta u \tag{3}$$

or

$$\Delta \begin{Bmatrix} \sigma_n \\ \tau_x \\ \tau_y \end{Bmatrix} = \begin{bmatrix} k_n(u) & 0 & 0 \\ 0 & k_{sx}(u) & 0 \\ 0 & 0 & k_{sy}(u) \end{bmatrix} \Delta \begin{Bmatrix} u_n \\ u_x \\ u_y \end{Bmatrix} \tag{4}$$

Where σ_n is the normal stress, τ_x and τ_y are the transverse stress in the x and y directions, respectively (see the coordinate system in Fig. 4). k_n, k_{sx} and k_{sy} are the joint stiffnesses in the normal (n) and shear directions (x, y), respectively. u_n is the normal deformation of the joint or joint closure. u_x and u_y are the shear deformations of the joint.

The variations of k_n with the joints closure can be obtained from joints closure tests as reported in reference [9], while k_{sx} and k_{sy} are expressed as [2]:

$$k_{sx}(u) = k_{sy}(u) = \frac{k_n(u_n)}{2(1+\nu)} \tag{5}$$

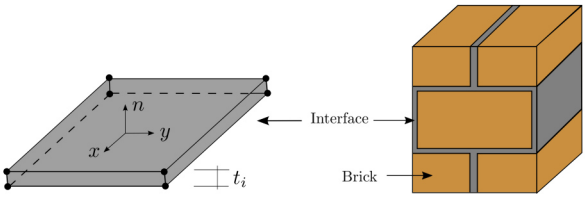

Figure 4: Schematic of RVE in pattern O showing the physical model, brick and interface.

The constitutive material model presented in Fig. 3 is implemented into Abaqus through a user material subroutine (UMAT) and, then, used to simulate refractory masonry walls subjected to different loading conditions at room and high temperatures.

RESULTS AND DISCUSSION

Biaxial loading and unloading at room temperature

In this test series, two refractory masonry walls with $1100 \times 1125 \times 140\,\mathrm{mm}^3$ dimensions were tested at room temperature. A 6 MPa biaxial compression load/unload was applied to the directions normal to bed and head joints. The FE model of the wall is presented in Fig. 5. The interactions between the contact surfaces of the wall, the plungers and the ground were considered in the FE model using frictional contact. The boundary conditions of the ground and the two fixed rigid plates are set to fully fixed.

Comparisons between the experimental and numerical force - displacement diagrams in the directions normal to bed and head joints during loading and unloading are presented in Fig. 6. It can be seen that the present numerical model can reproduce with reasonable accuracy the orthotropic displacement stiffening

mechanical behavior of the wall. The reaction force increases with the increase in the displacement due to the increase in material stiffness with gradual closure of joints. The maximum displacement in the direction normal to head joints is smaller as compared to that in the direction normal to bed joints, because the number of head joints is less than the number of bed joints.

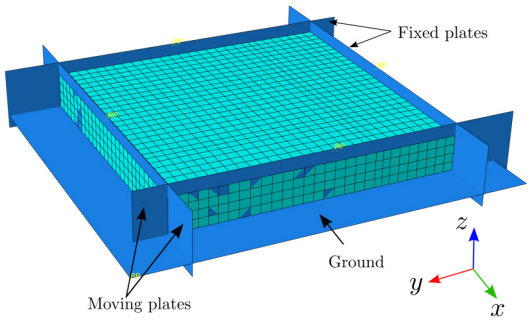

Figure 5: FE model of masonry wall.

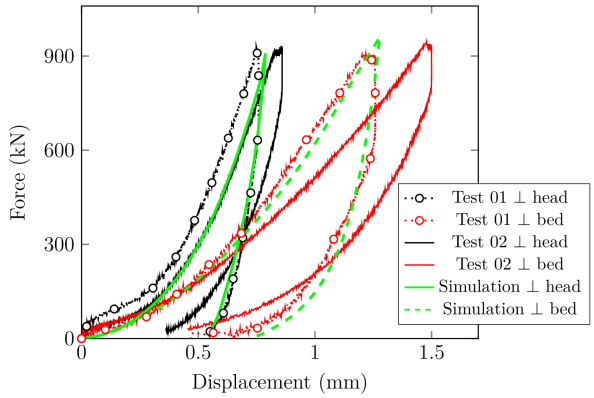

Figure 6: Comparisons between experimental (2 tests) and numerical force - displacement diagrams of the masonry walls subjected to biaxial compression loading/unloading at room temperature.

Biaxial creep behavior

In this test series, two refractory masonry walls with $1100 \times 1125 \times 140\,\text{mm}^3$ dimensions were tested at high temperature. The walls were heated up to 1500°C, then a constant biaxial compression load of 6 MPa was applied in the directions normal to bed and head joints. The temperature variations (with time) of the hot face (HF) and the cold face (CF) of the wall during heating and testing are given in Fig. 7. The five solid black lines represent the temperatures measured by the thermocouples in contact with the CF. The temperature fields of the wall as well as the deformed shape, by the end of the heating step, due to thermal expansion effects are given in Fig. 8.

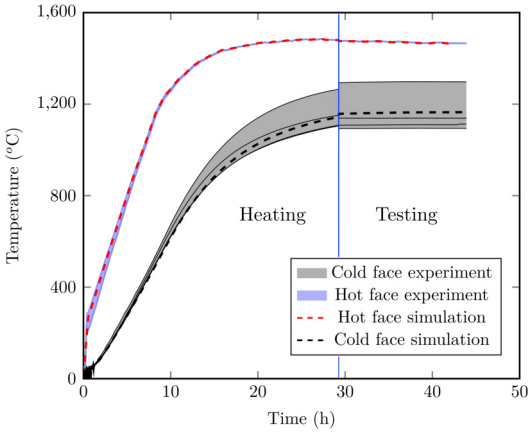

Figure 7: Time variations of the cold and hot faces temperatures during heating and mechanical testing.

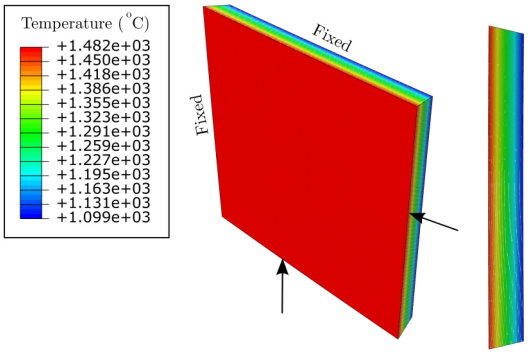

Figure 8: Temperature distributions of the masonry wall by the end of heating step showing the deformation of the wall due to thermal expansion.

The modeling technique of this test series are as following: firstly, transient heat transfer analysis have been carried out to compute the temperature fields during heating and testing. Then, the temperature fields are employed as

thermal loads in the transient thermomechanical analysis. The physical model of the thermomechanical analysis is the same as that reported in Fig. 5. During heating, load application, load holding and unloading steps, the boundary conditions of two fixed rigid plates and the ground are set to fully fixed. During heating, the two moving rigid plates were free to move then, during load application, load holding and unloading steps, the measured experimental reaction forces, in both directions, were applied as concentrated loads to the moving rigid plates.

Comparisons between the experimental and numerical displacement – time diagrams in the directions normal to bed and head joints during loading, holding and unloading steps are shown in Fig. 9. Good agreements between the experimental and numerical results can be observed. During load application step, and for both directions, an increase in the displacement due to the gradual closure of joints can be observed. The maximum displacement in the direction normal to bed joints is higher as compared to that in the direction normal to head joints due to the difference between the number of bed and head joints in the wall.

An example of the time variations of the stresses (from the end of heating step to the end of unloading step) in the CF and HF in the direction normal to bed and head joints (σ_{bed} and σ_{head}) are reported in Fig. 10. By the start of the loading step, the HF carries almost all the applied load due to the wedged deformed shape of the wall (shown in Fig. 8) caused by the thermal expansion and the temperature gradient through the thickness of the wall. With the increase of the applied load and the deformation of the zone near the HF, the contact area between the moving plungers and the sides of the wall started to increase and, therefore, the stresses in the CF as well. After reaching the maximum load level and due to the lower creep rate in the CF (due to the lower temperature) as compared to the HF, a decay in σ_{bed} and σ_{head} HF was observed due to stress relaxation. On the other hand, an increase in the σ_{bed} and σ_{head} CF was observed and, then, remained almost constant during the holding time.

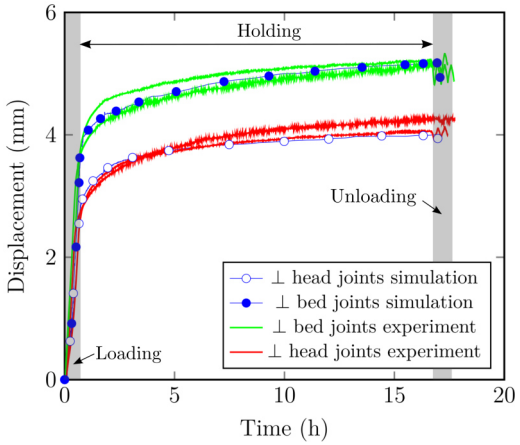

Figure 9: Time variations of the displacement in the masonry walls subjected to biaxial creep load at 1500 °C: experiments and simulations.

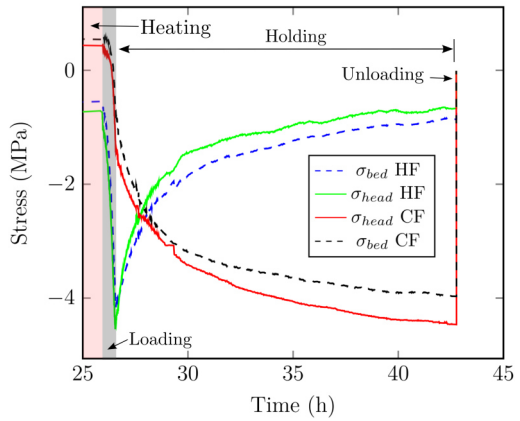

Figure 10: Time variations of the stresses in the masonry walls subjected to biaxial creep load at 1500 °C: simulation results.

Biaxial relaxation behavior

The goal of this series was to investigate the relaxation behavior of the wall (constant strain loading conditions). The modeling technique is similar to that of biaxial creep behavior (transient heat transfer analysis then, transient thermomechanical analysis). The physical model of the thermomechanical analysis is the same as

that reported in Fig. 5. During heating, the mechanical boundary conditions of the plungers and the ground are similar to those of biaxial creep behavior. During loading, the boundary conditions are almost the same as biaxial creep tests with only one difference, displacement boundary conditions were applied to the moving plungers and kept constant during the holding time.

Comparisons between the experimental and numerical time variations of the resulting reaction forces, in the directions normal to bed and head joints, during the two loading cycles are reported in Fig. 11. During loading (1st cycle), the resulting reaction forces increased gradually to reach around 600 kN. Then, when the position of the plungers is locked, a decay in the resulting reaction forces was observed due to the relaxation behavior of the wall. In the beginning of the holding stage, a significant decrease in the reaction forces can be observed. Similar behavior was noticed for both loading cycles.

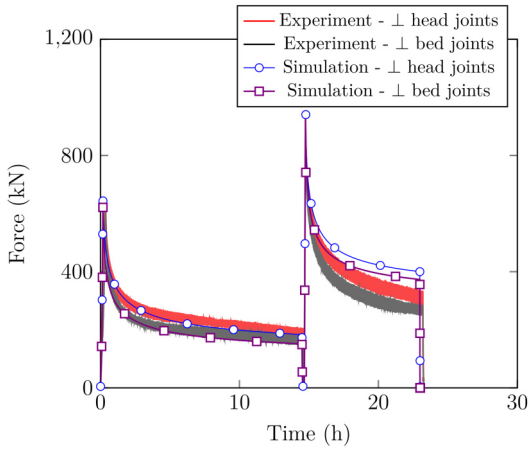

Figure 11: Time variations of reaction forces, in the directions normal to bed and head joints, in a masonry wall subjected to a biaxial relaxation loading conditions at 1500 °C: experiments (2 tests and two load/unload cycles) and simulations.

The joints patterns in the wall by the end of the holding step and after unloading of the two loading cycles are presented in Fig. 12. It can be seen that some joints reopen after unloading. In addition, the percentage of the closed joints in the second loading cycle (Fig. 12-c) is higher as compared to that of the first loading cycle (Fig. 12-a). This can be attributed to the higher load applied to the wall in the second loading cycle as compared to that of the first loading cycle.

CONCLUSION

This paper reports on large scale experimental characterization of refractory masonry with dry joints and computationally efficient multi scale models developed at University of Orleans - France. The multi scale numerical model of masonry with dry joints takes into account the highly nonlinear orthotropic elastic viscoplastic behavior of refractory linings with dry joints and accounts for the gradual closure and reopening of joints. The model has been used to predict the mechanical behavior of alumina spinel refractory masonry subjected to a wide range of loading conditions including: in-plane biaxial compression loading/unloading at room temperature, biaxial compression creep at high temperature and biaxial relaxation at high temperature. It has been shown that the developed numerical model can reproduce with reasonable accuracy the nonlinear orthotropic elastic viscoplastic behavior of masonry with dry joints and accounts for gradual closure of joints and joints reopening. This model may help in the design and optimization of large scale refractory masonry linings used in many high temperature applications such as steel ladles, rotary kilns and furnaces.

FUNDING

This work was supported by the funding scheme of the European Commission, Marie Skłodowska-Curie Actions Innovative Training Networks in the frame of the project ATHOR - Advanced THermomechanical multi-scale mOdelling Refractory linings 764987 Grant.

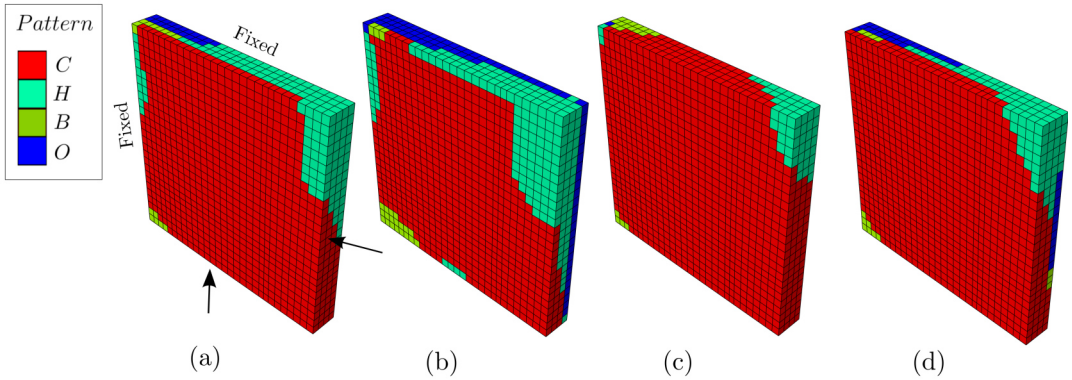

Figure 12: Joints patterns in a masonry wall subjected to biaxial relaxation: (a) after first loading, (b) after first unloading, (c) after second loading and (d) after second unloading.

ACKNOWLEDGMENT

M. Ali is thankful to R. Oliveira (University of Coimbra) and U. Marschall (RHI Magnesita - Leoben) for their contribution to the experimental tests.

References

[1] K. Andreev, S. Sinnema, A. Rekik, S. Allaoui, E. Blond, and A. Gasser, "Compressive behaviour of dry joints in refractory ceramic masonry," *Constr. Build. Mater.*, vol. 34, pp. 402–408, 2012.

[2] P. B. Lourenço, D. V. Oliveira, P. Roca, and A. Orduña, "Dry joint stone masonry walls subjected to in-plane combined loading," *J. Struct. Eng.*, vol. 131, no. 11, pp. 1665–1673, 2005.

[3] T. M. Nguyen, E. Blond, A. Gasser, and T. Prietl, "Mechanical homogenisation of masonry wall without mortar," *Eur. J. Mech. A/Solids*, vol. 28, no. 3, pp. 535–544, 2009.

[4] M. Ali, T. Sayet, A. Gasser, and E. Blond, "Computational homogenization of elastic-viscoplastic refractory masonry with dry joints," *Int. J. Mech. Sci.*, vol. 196, p. 106275, 2021.

[5] M. Ali, T. Sayet, A. Gasser, and E. Blond, "A Multiscale Model for Numerical Modelling of Homogenized Elastic-Viscoplastic Behavior of Mortarless Refractory Masonry Structures," in *14th World Congr. Comput. Mech. (WCCM), ECCOMAS Congr. 2020*, (Paris), 2021.

[6] M. Ali, T. Sayet, A. Gasser, and E. Blond, "Thermomechanical modelling of refractory mortarless masonry wall subjected to biaxial compression," in *UNITECR19*, (Yokohama, Japan), 2019.

[7] M. Ali, T. Sayet, A. Gasser, and E. Blond, "Transient thermo-mechanical analysis of steel ladle refractory linings using mechanical homogenization approach," *Ceramics*, vol. 3, no. 2, pp. 171–189, 2020.

[8] M. Ali, *Nonlinear thermomechanical modelling of refractory masonry Linings*. PhD thesis, University of Orléans - France, 2021.

[9] S. Allaoui, A. Rekik, A. Gasser, E. Blond, and K. Andreev, "Digital image correlation measurements of mortarless joint closure in refractory masonries," *Constr. Build. Mater.*, vol. 162, pp. 334–344, 2018.